

Mt. Amiata and the geothermal areas of Tuscany: Mt. Amiata, a quaternary volcano active between 0.3 and 0.19 Ma currently hosts a water-dominated geothermal field. It is located in southern Tuscany (Fig.1), about 70 km SE of the vapor-dominated geothermal field of Larderello-Travale, on the inner side of the northern Apennines. The area has been affected by extensional tectonics from the early-middle Miocene to the Present. Both geothermal fields have two known reservoirs: a shallow one (800-1000 m depth), no longer exploited, and a deeper one, exploited since the 80's, in the permeable carbonaceous horizons of the Tuscan Nappe and in the underlying metamorphic basement (depth 2500 - 4000 m), with temperatures in the range 300 - 400 °C. Mt. Amiata power plants have as of today an installed capacity of 88 MWe in the two areas of Bagnore and Piancastagnaio (Fig. 1).

The background regional heat flow (HF) of the whole coastal belt of Tuscany has average values of 100-120 mW m⁻². The HF anomaly peaks to 500-600 mW m⁻² at Mt. Amiata and 800-1000 mW m⁻² at Larderello (Fig. 2). Surface heat flow surveys carried out in an area close to the western flank of Mt. Amiata highlighted a strong thermal anomaly (Fig. 3); the continuation at depth of the geothermal features of the area is confirmed by the shape of the relative Bouguer gravity anomaly map (Baldi et al., 1995). Seismic surveys detected a regional high-amplitude discontinuous reflector with local bright-spot features, named "K-horizon". This horizon tops at about 3-4 km depth in correspondence of the Larderello and Mt. Amiata fields, deepening towards the peripheral areas. Recently, a second highly reflective horizon (K-2) was detected beneath the K-horizon, (7-9 km deep; 7 km in our model). Two deep seismic transects (CROP 18 A and B) significantly improved the knowledge of the crust underlying Tuscany (Figs. 2 and 5).

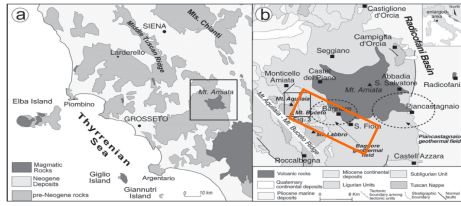


Fig. 1 - a) Generalized geological map of southern Tuscany. **b)** Geological sketch-map showing the Mt. Amiata geothermal region (see box in (a) for location). Orange box indicates the area under study. (From Brogi, 2008, modified).

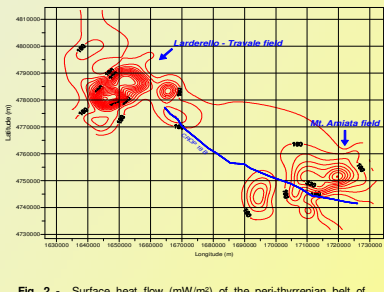


Fig. 2 - Surface heat flow (mW/m²) of the peri-thyrrhenian belt of Tuscany: Dense contouring highlights the geothermal fields of Larderello-Travale (NW) and Mt. Amiata (SE): data from over 350 gradient wells and deep geothermal wells drilled since mid 60's to late 90's. Blue line = track of the deep seismic reflection profile CROP 18 B (see Fig. 5).

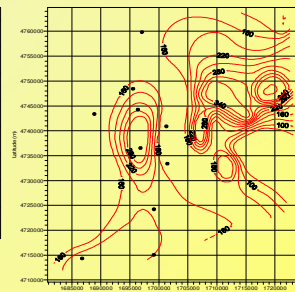


Fig. 3 Detailed surface heat flow (mW/m²) of the western part of Mt. Amiata geothermal field and adjacent areas. Black dots indicate geothermal gradient wells (150-200 m depth).

Modeling approach Coupled 2-D simulations of groundwater flow and heat transfer have been carried out with the HYDROTHERM 3.1 Interactive code (Kipp et al., 2008). Heat transfer mechanisms in the upper crust have been investigated by exploring the sensitivity on spatial variations of hydraulic and thermal properties of rocks. The geological setting has been schematized into four layers (see Fig. 5 for details). The model dimensions are: 30-34 km (width) by 8 km (depth). The model mimics most of the SE part of CROP 18 B profile (Fig. 4). The finite-difference grid consists of 6000 to 6800 nodal points. Grid cells are equally spaced all over the model, with internodal distances of 200 and 200 m along both the x and z directions (Fig. 5).

The lateral boundaries were treated as no-flow boundaries; the upper boundary as a no-flow, constant temperature (T) and pressure (P) boundary. Two different boundary conditions have been tested for the bottom of the model: i) no-flow, fixed temperature-pressure conditions, and ii) no-flow, specified heat flux (HF) conditions.

The values for boundary T, P and HF have been let to vary with both space and time in order to simulate the anomalous thermal input inferred at the bottom of the model (Table 1). Geothermal gradients vary between 35 and 50 °C km⁻¹.

Most of the reference data used to calibrate the model come from in situ (thermal profiles) and laboratory (thermal properties of rocks on core samples) measurements. On the basis of drilling results from literature, we assumed the formations belonging to the Reservoir block (Fig.5) to be characterized by the highest values of permeability (κ) and porosity (ϕ). In contrast, rocks from the Lower Basement and Basement layers are assumed to be less permeable and porous (Table 2).

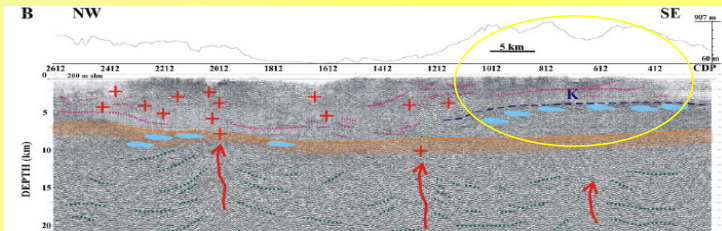


Fig. 4 - Interpreted post-stack depth migrated seismic line CROP 18 B (track in Fig.2). Dashed blue line: K-horizon. Orange line: K2-horizon. Pale-blue zones: fluid evidence. Red arrows: vertical channels. Red crosses: magmatic intrusions. Dotted pink lines: shallow reflections. Dotted green lines: deep reflections. Yellow oval: Mt. Amiata area. From Accaino et al. (2005), modified.

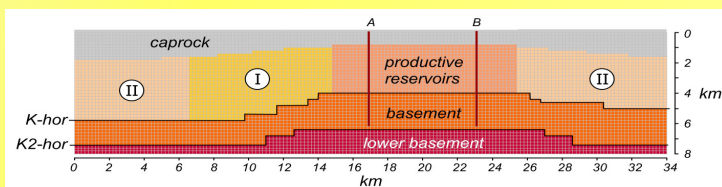


Fig. 5 - 2-D grid of the area under study, with lithological units and location of monitoring points A, B, I, II : geological formations adjacent to productive reservoir, belonging to the same lithological units, but with different hydraulic properties.

No-flow, constant T,P model						
T TOP	T BOTTOM	P TOP	P BOTTOM			
invariant	MIN	MAX	invariant	MIN	MAX	
15°C	450°C	600°C	1 bar	700 bar	900 bar	

No-flow, constant Heat Flux model						
T TOP	Heat Flux	P TOP	P BOTTOM			
invariant	MIN	MAX	invariant	MIN	MAX	
15°C	120 mW m ⁻²	1000 mW m ⁻²	1 bar	700 bar	900 bar	

Table 1 - Boundary conditions at the top and bottom of the domain

Results and discussion The permeability contrast between the three deeper layers turned out to be the most important parameter influencing the numerical output, and it underwent a sensitivity analysis (Table 2). Depending on the age of the Mt. Amiata volcanic activity (0.3-0.19 Ma; Brogi, 2008), the models were run to an average time period of 0.5 Ma, to encompass the magma chamber emplacement and the post-magmatic stage.

The results give two main scenarios:
 i) best fitting conditions between the numerical outputs and data from deep geothermal wells were achieved assuming relatively high permeability values ($\kappa_v > 5 \times 10^{-17}$ m²) in the Basement. This allows thermal convection to develop at depth greater than 4000 m b.g.l., while heat transfer in the above standing reservoir occurs mainly by conduction, with high temperatures but little convection (Fig. 6). This is in contrast with the occurrence of the productive geothermal reservoir (see logs A and B in Fig. 9);
 ii) efficient thermal convection develops within the productive reservoir when Basement and Lower Basement layers are modeled as scarcely permeable ($\kappa_v < 5 \times 10^{-17}$ m²). This effect is enhanced by the use in the basement lithological units of thermal conductivity values, λ , lower than 1.8 W m⁻¹ K⁻¹ (Table 2), consistent with the effect of high temperatures. Under these conditions, the basement shows almost no convective behaviour. The fitting between numerical outputs and data from deep geothermal wells appears though only partial in the reservoir, due to the asymmetric shape of the convection cell (Fig. 7 and logs A2 and B2 in Fig. 9).

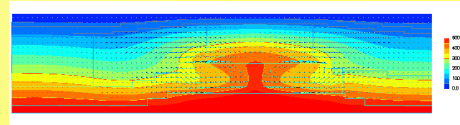


Fig. 6 - Thermal and water flow fields after 500 ka simulation time. No-flow, fixed T,P model, high-permeability Basement (reduced geometry, width = 30 km; depth = 8 km)

Fig. 7 - Thermal and water flow fields after 500 ka simulation time. No-flow, fixed T,P model, low-permeability Basement (extended geometry, width = 34 km; depth = 8 km).

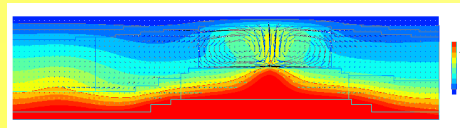
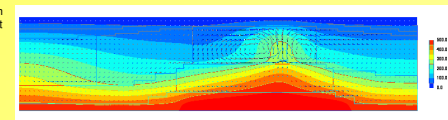


Fig. 8 - Thermal and water flow fields after 500 ka simulation time. No-flow, fixed basal Heat Flux, low-permeability Basement (extended geometry, width = 34 km; depth = 8 km).

Lithologic unit	porosity, ϕ		horizontal permeability, κ _h , m ²		thermal conductivity, λ, W m ⁻¹ K ⁻¹
	MIN	MAX	MIN	MAX	
Caprock	0.10	0.15	1 × 10 ⁻¹⁹	1 × 10 ⁻¹⁸	2.2
Productive Reservoir	0.15	0.20	1 × 10 ⁻¹⁶	5 × 10 ⁻¹⁵	f(T)
Reservoir, Unit I	0.15	0.20	5 × 10 ⁻¹⁷	5 × 10 ⁻¹⁵	f(T)
Reservoir, Unit II	0.10	0.15	5 × 10 ⁻¹⁷	5 × 10 ⁻¹⁵	f(T)
Basement	0.03	0.08	1 × 10 ⁻¹⁸	5 × 10 ⁻¹⁶	f(T)
Lower Basement	0.01	0.05	1 × 10 ⁻¹⁸	(invariant)	1.5

* = horizontal to vertical permeability ratio, κ_h/κ_v, between 5 to 20

Table 2 - Range of permeability, porosity, and thermal conductivity values assigned to the different lithologic units.

Conclusions The best fit between the modeling scenarios and the real conditions existing in the nearby reservoir of the Mt. Amiata geothermal fields envisages permeability values in the Basement and Lower Basement remarkably lower than in the above standing reservoir units: this allows the onset of a robust convection in the reservoir itself, with temperature values locally consistent with the data measured in deep geothermal wells.

Major results are as follows:
 i) Permeability contrast, both vertical and horizontal, appears to be the major control factor of the thermal and flow fields: a major source of uncertainty pertains to the poor knowledge of the spatial variability of this parameter
 ii) Results show a small dependence on a wide range of porosity variations
 iii) Heat transfer rate strongly depends on the thermal boundary conditions (bottom T or basal HF).

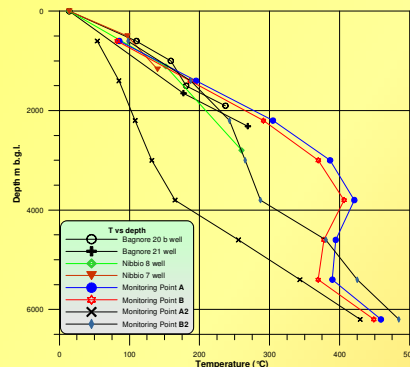


Fig. 9 - Comparison of the data measured in 4 deep geothermal wells close to CROP 18 B profile, with two sets of modelling results at the monitoring points A and B (model in Fig. 6) and A2 and B2 (model in Fig. 7).

REFERENCES:
 - Accaino F., Tinivella U., Rossi G. and Nicolich R., 2005. Geofluid evidence from analysis of deep crustal seismic data (Southern Tuscany, Italy). *Journal of Volcanology and Geothermal Research*, 148, 46-59.
 - Baldi P., Bellani S., Ceccarelli A., Fiordelisi A., Rocchi G., Squarci P., Tafti L., 1995. "Geothermal anomalies and structural features of southern Tuscany (Italy)". *Proceedings World Geothermal Congress*, 2, 1287-1291.
 - Brogi A., 2008. "The structure of the Monte Amiata volcano-geothermal area (Northern Apennines, Italy): Neogene-Quaternary compression versus extension". *Int. Journal of Earth Sciences*, 97-4, 677-703.
 - Kipp K.L. Jr., P.A. Hsieh and S.R. Charlton, 2008. "Guide to the Revised Ground-Water Flow and Heat Transport Simulator: HYDROTHERM -- Version 3". U.S. Geological Survey Techniques and Methods 6-A25, 160 p.